Point by point response (blue text) to reviewers' comments and suggested corrections (black)

Reviewer 1 (Major Revision)

The manuscript provides a comprehensive analysis of seismicity in Appenines in the area framed by the 2009 and 2016 Central Italy earthquakes. Three different precise location catalogs are combined and among others hypocenter migration, clustering and fault strength evolution are analyzed.

The paper brings variety of results which forwards our understanding of earthquake interaction in this area and relation between mainshock-aftershock sequences and swarms, however I am missing one-two main clear outputs. The missing main idea is also visible in the Abstract and Conclusions which highlight points that are not given in the main text, which is required for a research paper.

I recommend a major revision that would reshape the paper extracting one-two highlights and addressing the comments below.

Thank you for your suggestions to improve the focus of the paper and for your interest. We appreciate these observations. The two main points raised, as reflected in the abstract and conclusions, are now addressed with greater detail in formulation and methods on the two points below:

1. Variability of diffusivity within individual clusters**:** Our analysis shows that the migration velocity of the seismic fronts exhibits phases of pronounced acceleration, typically preceded by more controlled and stationary stages. In some cases, particularly for clusters of lower magnitude, these initial phases remain regulated, and the front does not propagate rapidly. This variability clearly indicates the inherent complexity of the fault system, including fault geometry and lithological heterogeneity, the latter beyond the scope of the present study.
2. Low effective stress drop**:** This characteristic, most evident in clusters with a higher number of events and greater energy release, suggests a significant aseismic contribution. Such an interpretation is consistent with the observed deficit between cumulative seismic moment, and geodetic moment. This point is closely linked to the first. Higher seismic front migration velocities and accelerations appear to be associated with fluids that influence fault strength promoting aseismic slip.

In revising the manuscript and supplementary material, we have also:

- Better clarified the formulations used to describe the potential reduction in fault strength associated with seismic front diffusivity, highlighting variations in seismic front migration;
- Detailed the methodology for calculating the effective stress drop;

These aspects were not sufficiently addressed in the initial version of the manuscript.

We trust that these revisions adequately address the reviewer's concerns and improve the clarity and rigor of the manuscript.

Comments

The chapter 2 gives describes the data (catalog) selection and mentions the slip deficit after the 2009 and 2016 sequences. This appears a bit out of scope of a data section; I guess it would better fit to Discussion. Moreover, the data analysis provided is not related to slip deficit of the analyzed sequences, so this part appears a bit superfluous.

We acknowledge that introducing the slip deficit in the data section may be misleading. However, we consider it relevant due to its close relationship with the low effective stress drop observed for the main clusters (as clarified in point 2 above). Following the reviewer's suggestion, we have moved this section to the *Diffusivity and Effective Stress Drop* paragraph. In the revised text, we clarify that the low effective stress drop values estimated for the clusters can be linked to the GNSS- and InSAR-derived seismic moment deficit (approximately 30–35%) relative to the deformation observed in areas surrounding the main events. This relationship implies a significant aseismic contribution, which we now address in the appropriate context.

Fig.2 y-label would benefit from indication SE and NW directions caption: what is the meaning of "The light blue and orange vertical segments indicate the extent of the coseismic ruptures " I do not see these segments in the figure fonts are too small

We added the indications and we improved the Figure 2 as requested.

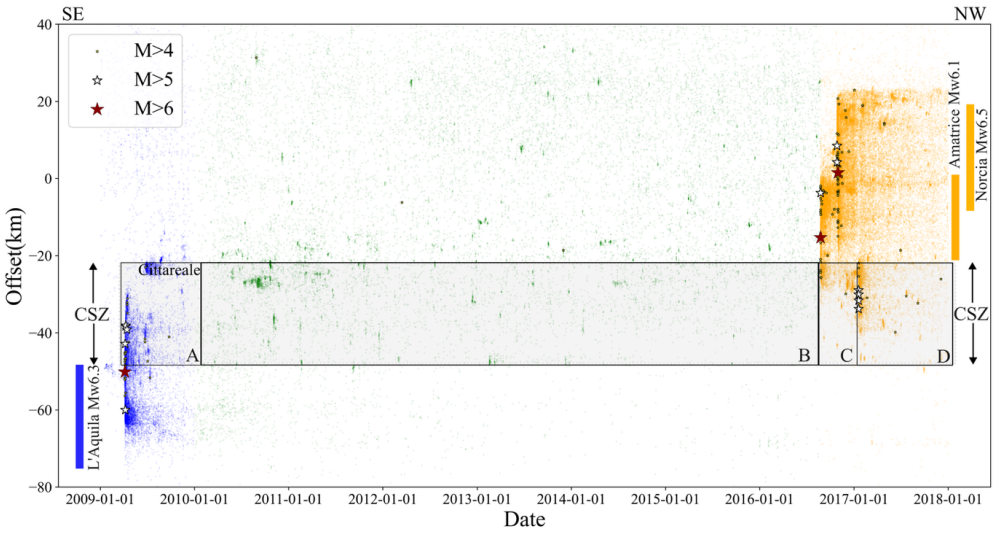

Figure R1 – Corresponding to Figure 2 in the main text

Fig. 3: fonts and symbols are extremely small. You may spare space e.g. by removing y-tick labels in the B,C,D lines and similar.

Modified as requested

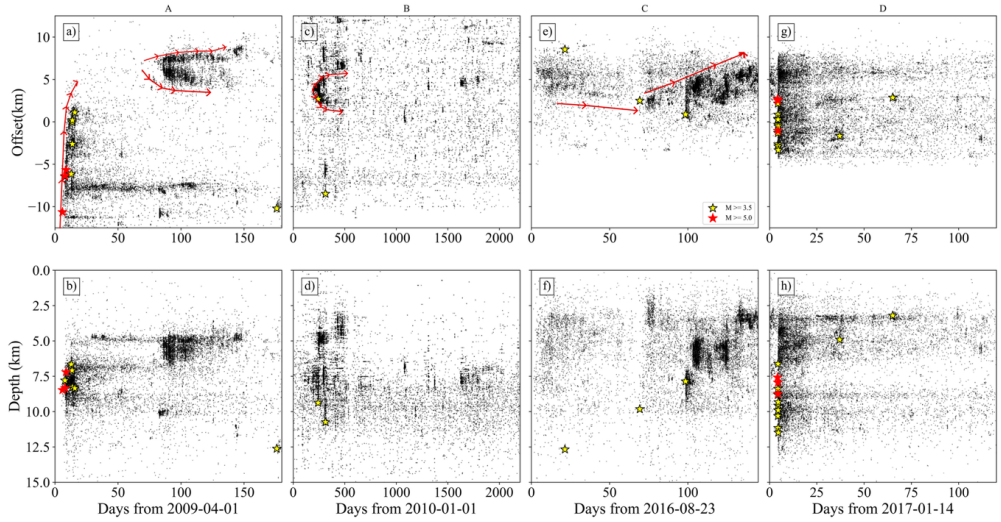

Figure R2 – Corresponding to Figure 3 in the main text.

Fig. S3: I like the representation of the ratio of seismicity before and after !

Thanks for appreciating Figure 3 that visualized the areas affected by changes in seismicity.

Fig. 4:the projection (x-axis in the lower row) is not described; I guess it is he grey line in the map views axes tick labels are too tiny

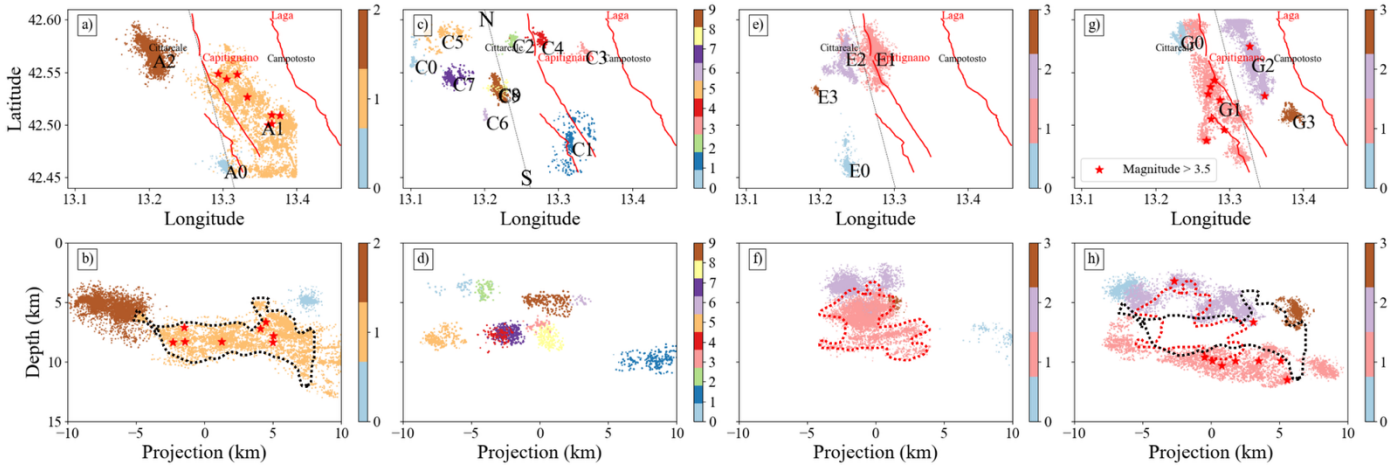

Figure R3 – Corresponding to Figure 4 in the main text

For figure 4 we increased tick labels size and specified in the caption that the projections are along the grey line (N-S) shown in top panels.

Table 2: It is not clear what does the 4th column labeled c.mag show; the caption names ‘magnitude’. I guess it is the Completeness magnitude. It should be clarified and also describe the method used for its determination.

This is the cutoff magnitude (the minimum magnitude within the cluster). Added in the caption.

Table 3: symbols for Static friction and Pore pressure coefficient should be given to make a link it to Fig 9 showing the symbols in the graph.

We provided in Tab. 3 the symbols used in Fig. 9

Fig. 7: fonts are too small

We increased the size of the fonts. The displayed velocity in km/day is the maximum velocity measured.

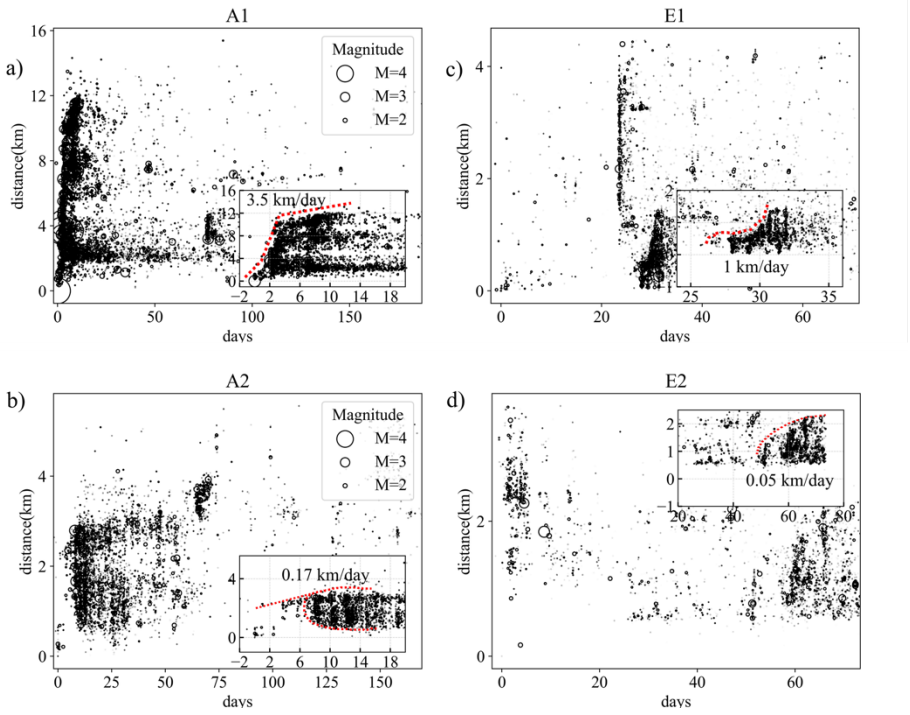

Figure R4 – Corresponding to Figure 7 in the main text

Fig. 9: For each friction coefficient a set of three lines is shown - how do the individual lines differ?

Curves of time (days) versus strength (MPa) are calculated using static friction coefficients (λ= 0.7, 0.8, 0.9). For each static friction coefficient, we present three curves with different initial pore pressures (μ_s= 0.65, 0.75, 0.85). The values of μ_s and λ are now indicated along the curves in Fig. 9

130: The sentence 'The strike parameters of the MW 5+ events of 2009 compared to those of 2017 indicate a slight plane rotation at depth where the dip is lower' is unclear as it appears to be related to Fig. S2 where strikes of M>3 earthquakes are shown and no depth dependance is plotted.

We agree about the unclear sentence and have corrected the text. Our observation relates to Locchi et al., where the centroid of focal solutions for all M>5 lies within a narrow depth range of 7 to 9 km. We observe that strike angles for M>5 range from 312 to 332 degrees, and dip angles from 38 to 71 degrees. For M>3 focal solutions slight rotations are observed from south to north in CSZ, as shown in Fig. S3 of the revised supplementary material.

211 Please explain what does it mean ‘the timing of the largest event (tm) normalized by the mean’.

In Zhang and Shearer (2016), the time of each event within the cluster is normalized $(t_i - t_{min})/(t_{max} - t_{min})$. We then calculate t_m, which is the ratio of the time of the largest moment magnitude event to the mean of the normalized times. This sentence is included in the text.

259 and below: The analysis of time evolution of diffusivity is quite unusual and deserves a brief explanation first also in the text (not only in the figure caption). I also find the diffusivity fits in Fig.8 c-e not justified as the higher diffusivity curves are supported by only few scattered points which might be location outliers.

We added a brief explanation to the main text, consistent with the caption. The curves shown are indicative and do not imply higher diffusivity values in Figures 8c–d. Additionally, we revised Figure 8 by increasing the tick label font size and removing the curves corresponding to higher diffusivity in Figures 8c-d.

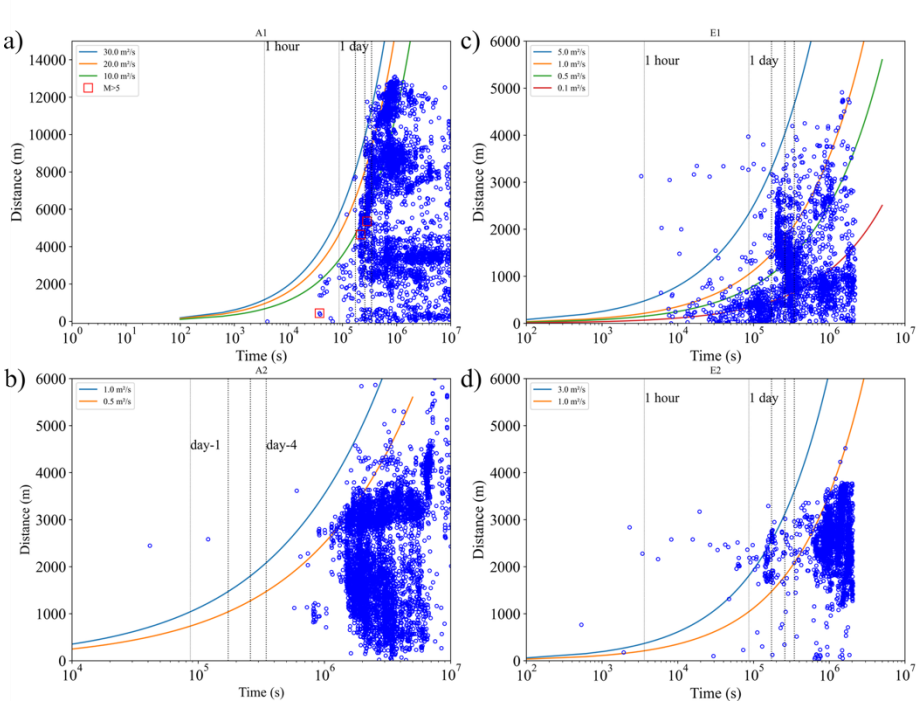

Figure R5 – Corresponding to Figure 8 in the main text

What does the swarm-like behaviour mean in this context? And how is it found that pore-pressure is limited? I feel this part is rather overinterpreted.

Figure 8a shows that the expansion of the seismic front is relatively slow during the first two days, with diffusivity around 10 m²/s. After this initial period, the diffusivity increases significantly, reaching approximately 30 m²/s. Similarly, as shown in Figure 7a inset, the migration velocity of the seismic front for the same cluster increases from about 1 km/day to 3.5 km/day after two days (insets of Figg. 7a and b are shown in detail below).

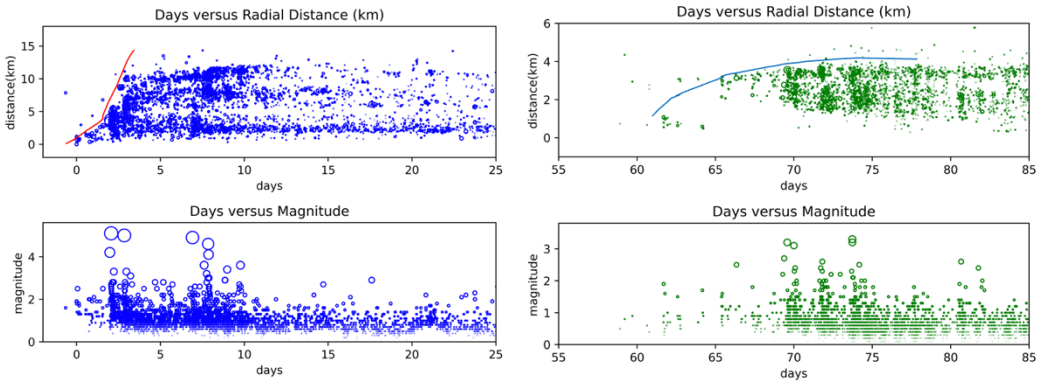

Figure R6 – (left panel) – A1 cluster with migration velocity increase from 1 km/day to 3-4 km/day in the first 5 days → high critical fault (self-sustained aseismic slip); (right panel) A2 cluster - migration velocity decrease from 200 m/day to lower than 100 m/day → low critical fault condition (De Barros et al., 2021).

De Barros, L., Wynants-Morel, N., Cappa, F., & Danré, P. (2021). Migration of fluid-induced seismicity reveals the seismogenic state of faults. *Journal of Geophysical Research: Solid Earth*, 126, e2021JB022767. **https://doi.org/10.1029/2021JB022767**

In the text we only highlight this observation to emphasize the change in propagation dynamics.

272: Please give the basic formulas used to calculate curves of static friction and pore pressure coefficient and explain. This is one of the main results of the paper and it is the not sufficient to refer to the Malagnini's papers; also the pore pressure coefficient (a ratio of pore pressure and lithostatic pressure) should be defined.

As requested, we add into the supplementary material a section including the basic formulas (derived from Malagnini's papers).

281: Similarly, it should be indicated how the effective stress drop was determined and give a reference - possibly Roland and McGuire (2009) or Fischer and Hainzl (2017)?

The effective stress drop was calculated under the assumption that all events within a cluster lie on a plane, following the formulation proposed by Fischer and Hainzl (2017). Specifically, we first estimated the total rupture area of each cluster and derived its equivalent radius. By summing the seismic moments of all events within each cluster, we then computed the effective stress drop using the Fischer and Hainzl (2017) approach. This method provides a consistent framework for evaluating cluster-scale stress parameters. The revised manuscript now explicitly cites Fischer and Hainzl (2017) as the reference for this calculation.

Reviewer 2 (Major Revision)

The paper describes in detail the spatio-temporal evolution of seismicity in the Campotosto (Italy) area between 2009 and 2017. This area is of interest because it lies between the regions affected by the 2009 L'Aquila and 2017 Central Italy seismic sequences. The work uses previously published high-resolution earthquake catalogues. The authors use HDBSCAN (Hierarchical Density-Based Spatial Clustering of Applications with Noise), a hierarchical density-based method, to detect clusters of seismicity within the area.

The paper is generally cogent and well written. However, Section 4, "Clustering Analysis", which forms the basis for the interpretation of results, requires further additions and clarifications. The figures are relevant but require minor changes to improve their clarity. Other sections contain minor inaccuracies that should be corrected or discussed. In summary, although there may not be substantial changes to the results, in my opinion, major revision is necessary before this paper can be accepted for publication.

I list my comments in the points below.

We appreciate the reviewer's interest and the identification of key inconsistencies requiring clarification. Below, we provide point-by-point responses aimed to refine the text and add details to improve clarity for readers.

We have added a section to the supplementary material discussing DBSCAN and HDBSCAN, two clustering methods that differ in their approach, parameter sensitivity, ability to handle cluster shape and noise, and output management. The supplement includes a comparison of these methods, while the main text highlights the rationale for selecting HDBSCAN. Specifically, HDBSCAN demonstrates superior sensitivity—up to 82% compared to DBSCAN's 50–62% (Hunt et al., 2021)—making it the preferred choice. Its ability to manage varying density environments and detect clusters across all density ranges is particularly advantageous for analysing heterogeneous datasets such as those in the CSZ.

Below are point-by-point clarifications based on the reviewer's suggestions.

Main points:

Completeness magnitude estimation

In section 2, lines 124–126, the authors state: “Figure S1 shows the frequency–magnitude distribution of the three catalogues. The completeness magnitude changes over the 9 years from 0.7 (Valoroso et al., 2013), and 0.4 (Sugan et al., 2023) to 0 (Waldhauser et al., 2021).” It is unclear how the completeness magnitude was estimated.

The maximum curvature method typically underestimates the completeness magnitude, so it is common practice to add 0.2 to the value estimated by this method. In this case, all maxima in the frequency–magnitude distribution are greater than 0, making a completeness magnitude of 0 unlikely.

Figure S9 in the supplementary material of Sugan et al. 2023 (reproduced below) presents histograms of templates (magenta) and new detections (light blue) from 2009 to 24 August 2016, across the area connecting L’Aquila and Amatrice. The completeness magnitude in this catalog is estimated by averaging two methods: the maximum curvature method (Wiemer and Wyss, 2000) and the b-value stability method (Cao and Gao, 2002). As shown in panel (b), the completeness magnitude approaches 0 during periods when significant clusters affected the area, while values of 0.4–0.5 are observed during intervals of reduced seismicity, such as between 2011 and 2012.

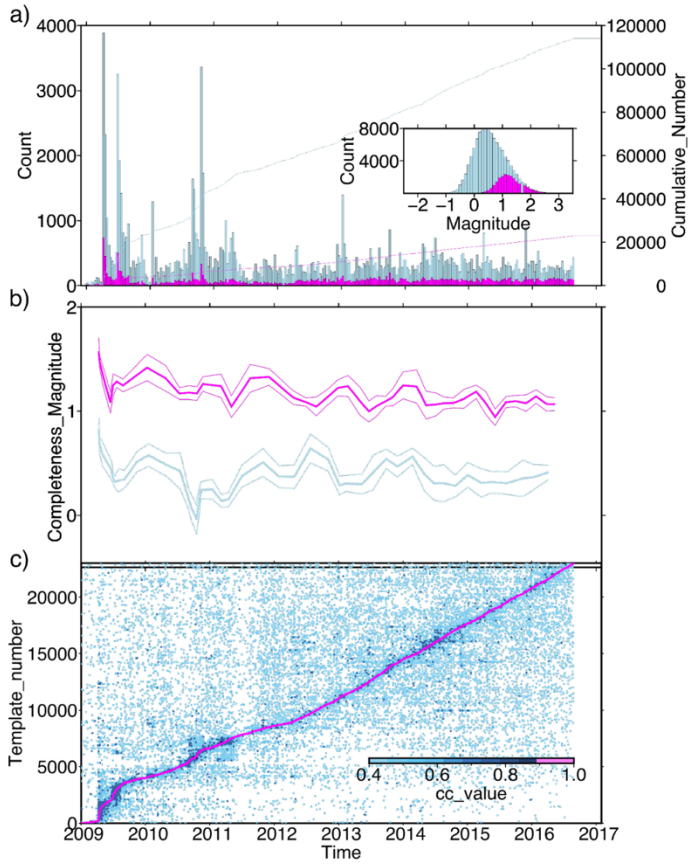

Figure R7, corresponding to Figure S9 in Sugan et al., 2023 shows:

a) Histograms of templates (magenta) versus new detections (light blue) from 2009 to 24 August 2016. The inset in a), also shows the number of events versus magnitude.

b) Completeness magnitude (Mc) of templates (magenta) and the augmented catalog versus time (light blue). Mc was calculated by averaging two methods, the maximum curvature method (Wiemer and Wyss, 2000) and the method based on b-value stability (Cao and Gao, 2002). Solid thick lines indicate the average value; thin lines represent plus or minus one standard deviation. A time window of 250 events with 50% overlap was used.

c) Time distribution of templates (magenta line) and associated new detections. New events are colour scaled according to the average cross-correlation value of detection. The diagram illustrates the ability of the templates to identify new events before and after the template itself.

Two further points should be considered: (1) template matching catalogues may have spatial "holes" if events occur where no templates are available, so the overall completeness magnitude may be underestimated because some less seismically active sub-regions are not included; (2) at these very low magnitude values, differences between night and day are significant due to anthropogenic noise. Mixing data from different time intervals and coverage areas produces numerical results that underestimate the true overall completeness magnitude. I suggest either removing this information from the paper, as it is not particularly relevant to the subsequent discussion, or retaining it with a more detailed justification of the results.

We acknowledge the reviewer's concern and clarify this point. It is correctly noted that, despite the high sensitivity of template matching and its ability to detect events hidden in noise, the resulting catalog could be biased in unsampled areas where seismicity is low. However, we do not rely on b-values or statistical indices, as the frequency–magnitude distribution can critically influence interpretations.

In this framework, the template catalog described in Sugan et al. (2023) comprises 23,003 events with local magnitudes (ML) ranging from 0.1 to 5.2, recorded within a 100 × 100 km² area between 1 January 2009, and the onset of the 2016 Central Italy sequence (August 24, 2016). Events were initially relocated using the NonLinLoc algorithm for absolute positioning. To further improve hypocentral resolution, a double-difference relocation scheme was applied using absolute travel times. The catalog coverage in the Campotosto area is nearly uniform, showing no significant spatial gaps in seismicity (see Fig. 1 in Sugan et al., 2023, red ellipse).

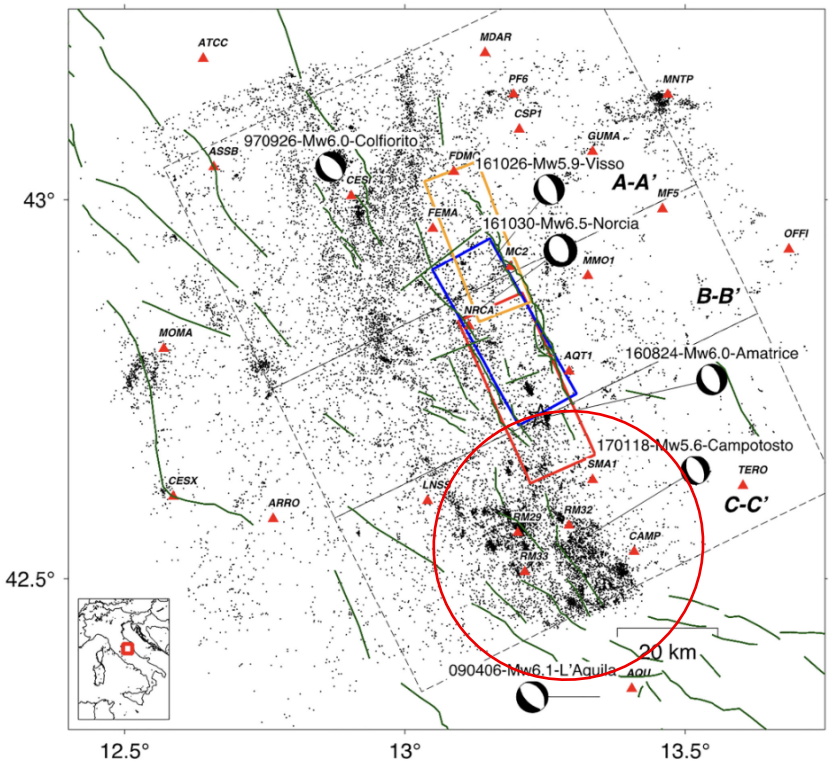

Figure R8 – Corresponding to Figure 1 in Sugan et al., 2023

Unlike other regions of Italy (such as the Po Plain region, which is significantly affected by high anthropogenic noise and exhibits clear diurnal variations in seismicity, Sugan et al., 2019), the study area does not show major day–night oscillations. Seasonal variations appear more pronounced (Figure R7b above). However, we acknowledge that this information is not directly relevant to the objectives of the present work. Following the reviewer's suggestion, we have removed this discussion from the manuscript to maintain focus and clarity.

Sugan, M., Vuan, A., Kato, A., Massa, M., & Amati, G. (2019). Seismic evidence of an early afterslip during the 2012 sequence in Emilia (Italy). *Geophysical Research Letters*, 46, 625635. **https://doi.org/10.1029/2018GL079617**

In Table 2, there is a field named c. mag; please define what this refers to. If it means completeness magnitude, my suggestions for section 2 also apply here.

It means cutoff magnitude (the minimum magnitude into the cluster). We specified it in the caption.

Clustering method. The authors used the HDBSCAN method to detect seismicity clusters. This hierarchical density-based method is an innovative technique in seismology and, in my opinion, should be described in detail to ensure

reproducibility of the results. Even if the code is available online, some basic points may be useful for readers who are not experts in density-based methods or are unfamiliar with this particular method.

I suggest some possible questions to address in the text. What are the differences between DBSCAN and HDBSCAN? How does this affect the number of input parameters?

We have added a section to the supplement, discussing DBSCAN and HDBSCAN, two methods with different clustering approaches, parameter sensitivity, handling of cluster shape and noise, and output management. In the supplement, we report the comparison by Hunt et al., (2021) and highlight in the main text the reasons why we preferred to use HDBSCAN.

Regarding the different approaches to the problem, DBSCAN performs flat clustering and identifies clusters based on density, labelling points as core, border or noise. In contrast, HDBSCAN constructs a hierarchy of clusters and extracts the most stable ones. HDBSCAN traduces the number of critical input parameters and improves robustness by eliminating the need to define the eps radius parameter. The comparison between DBSCAN and HDBSCAN highlights their respective strengths and limitations and the choice between them depends on the specific application requirements and data characteristics.

DBSCAN offers clear advantages with its high specificity and precision. This makes DBSCAN particularly suitable for limited blind searches and situations where falsely identifying non-existent clusters is more problematic than missing some true clusters (deBerg et al., 2017). HDBSCAN's superior sensitivity of up to 82% compared to DBSCAN's 50–62% (Hunt et al., 2021) makes it the stronger choice. Its ability to handle varying density environments and detect clusters across all density ranges is especially beneficial for analyses of heterogeneous datasets as in CSZ. While the original DBSCAN was sensitive to parameter choice, theoretical advances have shown potential for much reduced sensitivity. HDBSCAN's parameter setup has been described as easier and more intuitive, though careful parameter selection remains necessary to balance sensitivity against false positive rates (Hunt et al., 2021).

Mark de Berg, Ade Gunawan, and Marcel Roeloffzen, 2017. Faster DBScan and HDBScan in Low-Dimensional Euclidean Spaces. In 28th International Symposium on Algorithms and Computation (ISAAC 2017). Leibniz International Proceedings in Informatics (LIPIcs), Volume 92, pp. 25:1-25:13, Schloss Dagstuhl – Leibniz-Zentrum für Informatik (2017) https://doi.org/10.4230/LIPIcs.ISAAC.2017.25

Hunt, E. L. and Reffert, S., 2021. Improving the open cluster census. Astronomy & Astrophysics, 646:A104, February 2021.101, doi: 10.1051/0004-6361/202039341.102

Are the spatial and temporal dimensions simply normalized between, for example, 0 and 1, or are they scaled differently?

Normalization is necessary to give equal weight to different dimensions when time and space are considered together. We specified this in the revised manuscript. We also tried a different (two-step) approach, first clustering events in time, and then in space, obtaining comparable results. Thanks for asking for clarification.

How is the silhouette score defined, and what does it indicate?

Using the silhouette score for tuning, makes HDBSCAN more automated, but it also adds complexity. Instead of managing one parameter (min_cluster_size), you must handle a range of parameters and an evaluation metric. This is common in model selection workflows. Therefore, we used the silhouette score to identify the optimal number of clusters (for example, higher silhouette score usually indicates better clustering). The Silhouette Coefficient is calculated using the mean intra-cluster distance (a) and the mean nearest-cluster distance (b) for each sample. The Silhouette Coefficient for a sample is *(b - a) / max (a, b)*. Here, b is the distance between a sample and the nearest cluster to which the sample does not belong. Note that the Silhouette Coefficient is only defined if the number of labels satifies 2 <= n_labels <= n_samples - 1(https://scikit-learn.org/stable/modules/generated/sklearn.metrics.silhouette_score.html). We have added a clarification in the supplementary material.

Finally, what is the minimum number of events selected? In addition, a figure showing the silhouette score should be included to illustrate how the parameter "Number of events" is optimized.

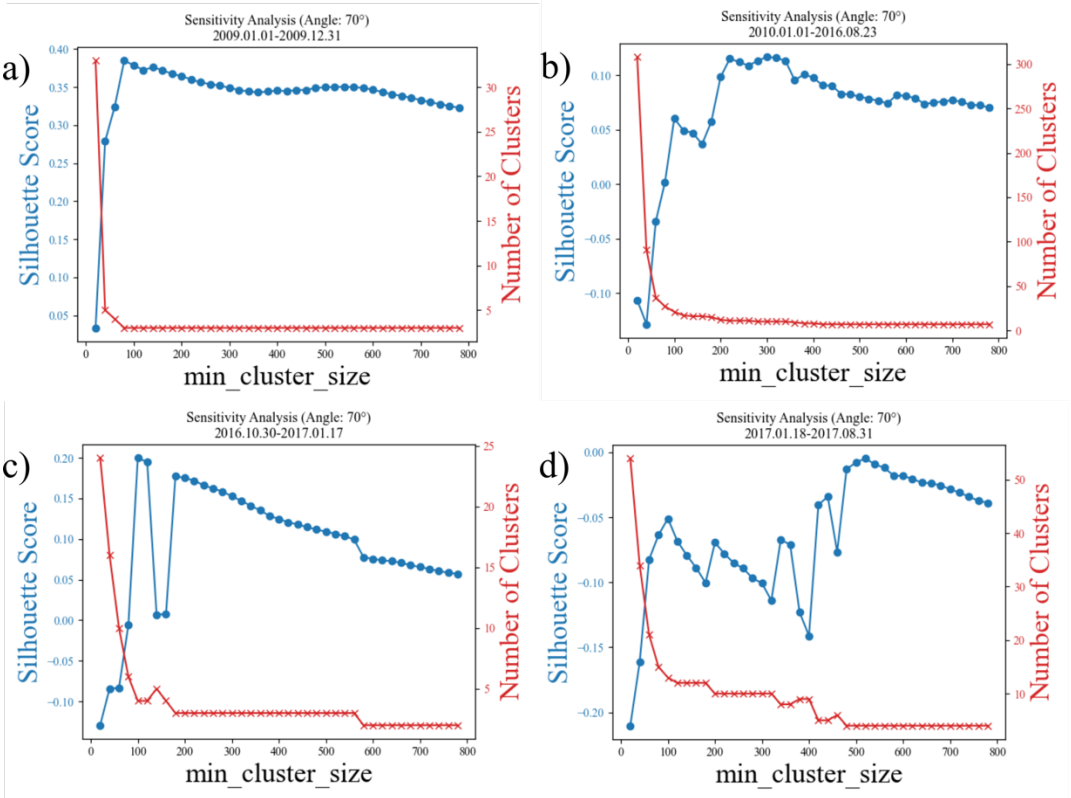

Figure R9 has been added to the supplement. We present the minimum cluster size versus the silhouette score for the time windows specified in Table 1. To determine the optimum number of clusters, we iterate the calculation of the silhouette score from 20 to 800 events in steps of 20.

Plan of orientation of the clusters. I do not understand why the orientation planes of the clusters have been estimated using convex hulls rather than PCA. Any clustering method may include some spurious background events in the clusters. In DBSCAN-derived methods, if time and space are analyzed together, such incorrect assignments may occur for events that are far apart in space but very close in time to those in the cluster. These events are at the border of the cluster. Analysis using convex hulls gives importance to events on the border of the cluster, which could result in inaccurate plane estimates. The authors claim that the difference between this approach and PCA is of the order of 70–490 m, but they also state that the estimated migration velocity in some cases is of the order of meters per day. Therefore, this difference may be significant. This part should be analyzed in greater detail. I also suggest providing the information on plane orientation in terms of angles, not only in meters (I assume meters at the cluster's border).

Thank you for raising this point, as we realised that clarification in the main text is necessary. The original statement was unclear and also incorrect. The convex hull is used to delimit the cluster volume and to estimate the in-plane area required for calculating the effective stress drop. The fault plane orientations shown in Figure 6 were determined using Principal Component Analysis (PCA).

For example, in cluster A1, the figure illustrates the variance distribution along the two principal in-plane directions: approximately 72% of events align with PC1 and 28% with PC2. The third component (PC3), representing the out-of-plane direction, exhibits minimal variance. The average orthogonal distance of some events from the planes, considering all clusters, ranges from 70 m to 490 m. We have corrected the statement in the main text accordingly and appreciate the reviewer's attention.

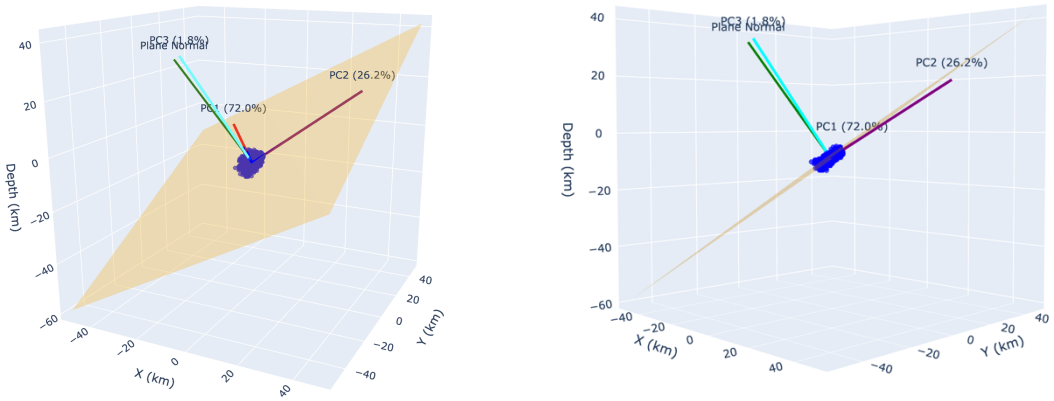

Figure R10 – PCA components with variance along the three orientations. We further verified that the projection of the identified planes at the surface generally follows the strike orientation of the main fault system. The figure is included in the supplementary material as Figure S6

The PCA components for each cluster are shown in the table below. In most cases, PC1 and PC2 together explain more than 80% of the variability, indicating that the distribution of points within each cluster is largely confined to a two-dimensional plane. The third component (PC3) contributes very little (often less than 10%), which means the data are nearly flat in three-dimensional space. This observation provides a basis for estimating the effective stress drop and supports the conclusion that the clusters developed along the main tectonic fault segments.

The PC1 angle in the table represents the orientation of PC1 relative to North. Comparing the PC1 angles of clusters A1 and A2 (2009 sequence) with those of G1 and G2 (2017 sequence) reveals an approximate 15° rotation towards North. In contrast, the PC1 of clusters that preceded the 2017 reactivation (E1 and E2) is already aligned with North. These rotations highlight the segmentation of the fault system.

Cluster	PC1(%)	PC2(%)	PC3(%)	PC1angle(°)
A0	50.70	36.20	13.10	99.62
A1	71.99	26.21	1.81	-35.54
A2	71.68	17.85	10.47	-33.51
C0	77.45	20.43	2.12	7.47
C1	63.39	29.81	6.80	-3.80
C2	68.21	27.28	4.51	-144.04
C3	69.25	23.67	7.08	132.66
C4	45.62	35.82	18.56	-15.45
C5	45.16	36.36	18.49	65.77
C6	65.08	29.67	5.24	-17.14
C7	59.26	28.84	11.90	132.52
C8	63.90	18.88	17.21	-63.25
C9	79.99	13.83	6.19	-22.00
E0	79.18	14.92	5.90	-5.61
E1	55.89	39.04	5.08	7.37
E2	71.32	23.56	5.12	1.65
E3	58.21	34.23	7.56	23.37
G0	68.23	17.28	14.48	10.08
G1	89.11	8.91	1.98	-20.94

G2	89.45	8.16	2.39	-21.53
G3	59.31	31.24	9.45	65.00

Table R1 – Cluster variance along the three PCA components and PC1 angle measured clockwise from the North. (The table is added to the supplementary material)

Cluster classification. In Figure 5, the clusters are classified as either swarm, mixed, or Mainshock-Aftershock using the approach of Zhang and Shearer (2016). However, it is unclear how this classification has been incorporated into the subsequent interpretation. For example, cluster E2 is identified as a Mainshock-Aftershock cluster, while cluster A2 is identified as a swarm. Yet, in the discussion on diffusivity, the authors state that both clusters (page 12, lines 265–266) exhibit swarm-like behavior. In my opinion, this inconsistency should be addressed in the discussion.

The classification by Zhang and Shearer is statistical; it does not directly reveal the underlying physical mechanism (such as fluid migration or stress transfer). It may be useful to provide a general overview of all clusters that typically are around a skewness value close to zero (symmetric distribution of magnitude with time). The boundaries separating different fields can vary from case to case, and mixed or complex sequences may be misclassified.

In the original version of the manuscript we stated: “This classification framework allows first-order analysis of clusters; most of them show an almost symmetric distribution of magnitude over time (skewness close to 0) and variable timing of the main event, with few clusters in the M-A range.”

The reviewer is correct in highlighting the inconsistency regarding the E2 cluster. To clarify this point, we show in the figure below the time-magnitude distribution of E2 (see the bottom panel). As can be seen, E2 is a complex cluster (the skewness and normalized time refer to the maximum magnitude event at the beginning of the sequence). Considering the temporal continuity of the events and the magnitude distribution, it can be defined as a swarm. We have added text on this point to provide more detail on the limitations of the classification.

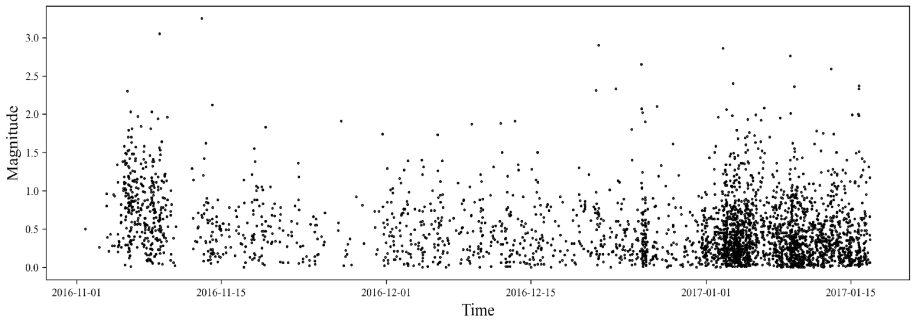

Figure R11. Time-Magnitude characteristics of seismic cluster E2.

Minor points:

Page 2, line 43: I suggest changing “15 years” to “20 years”: the L’Aquila earthquake occurred 16 years ago.

Corrected

Pages 2–3, lines 57–75: These lines appear to have been added later, interrupting the flow of the text, which perhaps previously moved from the current line 57 (midway) to line 76. The term CSZ is used here but is only defined at line 76, which disrupts the discussion. I suggest integrating this section more smoothly into the text and defining CSZ at its first occurrence.

We agree and restructure the Introduction, changes are shown in the tracked version.

Page 4, line 108: I suggest moving Table 1 and its reference here, so the reader can immediately see the years involved while reading the text.

Table 1 is moved as requested

Figures 4, 5, 6b, 10: The cluster names are often superimposed and difficult to read. To improve the figures, the text should be shifted slightly to enhance legibility.

Fig. 4, 5 and 10 are modified to allow clear clusters’ labels. Fig. 6b is left unchanged.

Page 8, line 213: In my opinion, the sentence “we use two key metrics: the timing of the largest event (tm) normalised by the mean, and the skewness value (μ). The skewness of moment release over time for a given sequence is calculated as in Roland and McGuire (2009).” should be rewritten for clarity. I assume that, to calculate tm for each cluster, the authors subtract the time of the first event from each event’s time, estimate the mean of these transformed times, and then divide the transformed time of the largest event by such mean. This process should be explained more clearly. If there is more than one event with the maximum magnitude, is the first chosen?

We modified the sentence as requested into: The skewness ($\mu 3$) of moment release for a given sequence is calculated as in Roland and McGuire (2009). We combine $\mu 3$ with the normalized time t_m as in Zhang and Shearer (2016). The time of each event (t_i) within the cluster is normalized $(t_i - t_{min})/(t_{max}-t_{min})$. Then we calculate tm as the ratio between

the time of the largest moment magnitude event and the mean of the normalized times. If there is more than one event with the maximum magnitude the first one is chosen.

Hopefully this statement is clearer.

When introducing the skewness value, it should be specified immediately what it refers to, otherwise it may be interpreted as the skewness of the time distribution. I also suggest using a different symbol for skewness, such as γ1, g1, or μ3, since μ is usually used for the mean. This change should also be made in Figure 5.

We also changed Figure 5 and assumed $\mu 3$ as skewness

Page 10, line 236: There may be a typo. I suggest "could not be measured" instead of "could not be measure".

We modified the sentence. "Some clusters exhibit ambiguous behavior with multiple phases, alternating between mainshock–aftershock sequences and swarm-like patterns. For these clusters, it is difficult to determine the velocity of the seismic front"

Page 10, lines 249–257: For clusters A1 and A2, the migration velocity is specified. For clusters E1 and E2, however, it changes over time. For the sake of symmetry, details on its variability and the range of variation (or the mean velocity) should be provided for these clusters as well.

We show in Figure7 insets the maximum velocity of the seismic front we can measure. These clusters exhibit ambiguous behavior with multiple phases, alternating between mainshock–aftershock sequences and swarm-like patterns.

Page 11, line 262: Perhaps D ~ 30 m²/s?

Modified.

Page 12, Table 3 caption: There is a typo: "Malagnini et al. (2010))".

Corrected.

Page 14, Figure 10: Please specify the units for cumulative seismic moment.

Units specified.